This article has been accepted for publication in a future issue of this journal, but has not been fully edited. Content may change prior to final publication. Citation information: DOI 10.1109/TWC.2018.2801803, IEEE Transactions on Wireless Communications

RFID Backscattering in Long-Range Scenarios

Francesco Amato, *Member, IEEE,* Hakki M. Torun, *Student Member, IEEE,* and Gregory D. Durgin, *Member, IEEE*.

***Abstract*—This work presents a 5.8 GHz RFID tag that, by exploiting the quantum tunneling effect, significantly increases the range of backscatter radio links. We present an electronically simple *Tunneling RFID Tag* characterized by return gains as high as 35 dB with link sensitivity as low as -81 dBm. Without relevant increase in power consumption, the Tunneling Tag enables a host of new wireless sensors and Internet-of-Things (IoT) applications that require both the long range of conventional wireless links and the low power consumption of semi-passive RFID devices. Selected measurements demonstrate a reader-to-tag separation distance 10 times higher than the maximum range of ideal semi-passive tags. Moreover, the collected experimental results allowed to outline a mathematical model demonstrating how the long-range RFID tag prototype can achieve distances unusual for this technology.**

***Index Terms*—RFID; reflection amplifier; tunnel diode; low-powered RFID; long-range backscattering; backscattering; modulation factor; tunneling tag; tunneling reflector; IoT; internet of things.**

I. Introduction

By 2020 there will be 200 billion of connected "Internet-of-Things" (IoT) devices [1] that will use wireless technology to communicate among each other and to human operators. Although the total global worth of IoT technology could be as much as 6.2 trillion USD by 2025 [2], the energy consumption and the need to replace batteries are serious obstacles to this optimistic deployment. Currently, a BLE module used in IoT applications requires 10.8 mW [3] to communicate; if operating one third of the time, a coin cell battery-assisted module[1] will consume more than 50 batteries per year. If those batteries will need to be replaced upon discharge, they will contribute to a volume exceeding 10,000,000 m^3 in electronic waste, filling up a space bigger than the volume of 9 Empire State Buildings[2] m^3 *per year*.

Backscattering communication through RFID nodes is a promising solution to solve the IoT energy burden of the future, but this technology is still limited in range and is not currently competitive with the wider coverage areas of BLE, WiFi, cellular and LoRa networks. Several steps have been undertaken among the research community to overcome backscattering communication limits. A joint design of reader and tag signals [5] as well as space-time coding [6] were suggested to improve both the performance of indoor scenarios, affected by multipath fading, and the reliability of MIMO backscatter RFIDs. Researchers in [7] have highlighted the need of an increased UHF bandwidth for accurate positioning and ranging with RFIDs, but only a few experimental results demonstrating the long-range potential of RFID transponders have been reported thus far.

This work extends the results shown in [8]. It demonstrates how a quantum tunneling-based RFID tag achieves free-space long-range backscattering communication links as wide as 1.2 km and presents a simulation tool to assist a system engineer in designing these links. The tool was tested by identifying possible scenarios where the *Tunneling Tag* would be beneficial. The modulation and long-range capabilities of the Tunneling Tag are experimentally demonstrated through an extensive measurement campaign (Fig. 1).

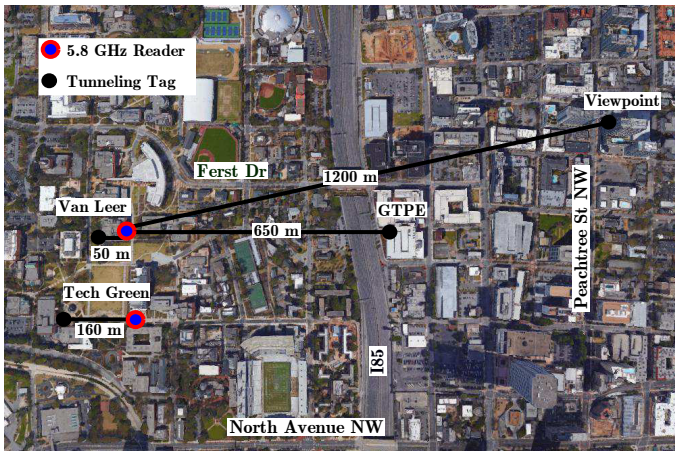

Fig. 1: Satellite view of the Georgia Tech campus and the Midtown neighborhood in Atlanta, GA (USA) showing locations and distances covered during the backscattering measurement campaign described in this work.

II. Rationale

To improve the range r of backscattering communications characterized by the following link budget equations:

$$P_t = P_T G_{tx} G_t \frac{\lambda^2}{(4\pi r)^2} \tag{1}$$

$$P_r = P_t G_t G_{rx} \frac{\lambda^2}{(4\pi r)^2} M, \tag{2}$$

a system engineer can operate on some parameters. Both the tag transponder and the reader sensitivities can be improved so that the former can activate its circuitry with lower levels of impinging power P_t while the latter can detect lower levels of received backscattered powers P_r; moreover, the

Francesco Amato is with the Sant'Anna School of Advanced Studies, Pisa, Italy, (email: francesco.amato@santannapisa.it)

Hakki M. Torun and Gregory D. Durgin are with the Georgia Institute of Technology, Atlanta, USA, (email: {htorun3, durgin}@gatech.edu).

Manuscript received April 6, 2017; revised September 19, 2017; accepted January 29, 2018.

This work was sponsored in part by NSF Grant CCSS-01408461.

[1]Coin cell battery capacity: 0.22 Ah, voltage: 3 V, volume: 1 cm^3.

[2]Empire State Building Volume: 1,047,723 [4].

This article has been accepted for publication in a future issue of this journal, but has not been fully edited. Content may change prior to final publication. Citation information: DOI 10.1109/TWC.2018.2801803, IEEE Transactions on Wireless Communications

gains of both the transponder antenna G_t and the reader receiving antenna G_{rx} can be increased; additionally the tag transponder loads can be chosen so that its modulation factor, $M = \frac{1}{4}\left|\Gamma_1 - \Gamma_2\right|^2$, can achieve values greater than 1. Limits are imposed on both the transmitting power P_T and the transmitting antenna gain G_{tx} of the reader whose maximum EIRP must be 36 dBm [9].

Despite the absence of limitations on the modulation factor M, its maximum value is typically 1 (in ideal semi-passive transponders). $M > 1$ is obtained by equipping the tag with active loads, such as tunnel diodes, that require some biasing power. Tunnel diodes can be used for different applications [10]: besides behaving like a Schottky diode when large biases are applied, a heterostructure backward tunnel diode can be used for energy harvesting applications [11]. Finally, the decreasing current as effect of the increasing bias gives to the tunnel diode a natural negative differential resistance $-R$ that can be used to design a *Tunneling Reflector* (TR). A TR was chosen as a valid microwave active load that significantly improves M without a relevant increase of the biasing power requirements [12]. The TR is based on a tunnel diode that, when properly biased, displays a natural negative differential resistance $-R_L$. When the TR is properly matched to an impedance Z_A, the corresponding reflection coefficient Γ becomes negative and greater than 1:

$$|\Gamma|^2 = \left|\frac{Z_L - Z_A}{Z_A + Z_L}\right|^2 = \left|\frac{R_A + R_L}{R_A - R_L}\right|^2 > 1, \tag{3}$$

making the modulation factor M greater than one. Of course, the law of conversation of energy is preserved since the TR converts the applied dc bias into RF power.

Upon backscattering, the base-band signal received on an RFID reader is given by:

$$V_{bb} = V_{dc} + V, \tag{4}$$

where V_{bb} is the base-band received signal, V_{dc} is the received dc component and $V = V_I + jV_Q$ is the time-varying signal. The desired modulated-backscatter data can be extracted from the base-band signal by blocking V_{dc} with a series capacitor. Since environmental and reader noise affect the quality of the wireless link, V can be measured as the average of N bursts received over a period of time.

To measure the signal-to-noise ratio of the backscattering link, the modulation error ratio (MER) can be used. It takes into account both the average of all the received symbols $|V|$ and the average error magnitude $|e|$:

$$|e| = \sum_{n=1}^{N} e_n = \frac{1}{N}\sum_{n=1}^{N}\sqrt{(V_I - V_{I,n})^2 + (V_Q - V_{Q,n})^2}. \tag{5}$$

The MER, in dB, is defined as:

$$MER = 20\log_{10}\left(\frac{\sqrt{V_{I,n}^2 + V_{Q,n}^2}}{\sum_{n=1}^{N}\sqrt{(V_I - V_{I,n})^2 + (V_Q - V_{Q,n})^2}}\right), \tag{6}$$

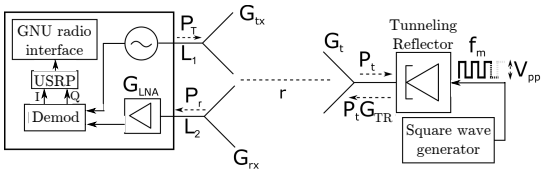

Fig. 2: Reader [13] and tag configuration used to collect the experimental data; details are listed in Table I. The homodyne receiver extrapolates the I and Q channels and passes them to the USRP. Data are acquired with the GNU radio interface, saved as **.bin* files, and made available on line [14].

where V_I and V_Q are the in-phase and quadrature average components of the received, demodulated symbol; $V_{I,n}$ and $V_{Q,n}$ are the quadrature components of the received, demodulated n-th symbol; and N is the total number of the received symbols.

III. The Experimental Setup

To test the backscattering capabilities of the prototype, the experimental setup in Fig. 2 was used. It consists of a reader and a Tunneling Tag tuned at 5.8 GHz. The tag is placed at different distances r from the reader that collects and processes the backscattered data.

A. The Microwave Reader

The fabrication of an early version of the 5.8 GHz microwave homodyne reader available at the Propagation Group Laboratory is documented in [13]. Its transmitting section generates a 5.8 GHz CW of power P_T and it is connected to an output antenna with gain G_{tx}. Its receiving section has a high-pass cut-off frequency of 20 kHz and a low-pass cut-off of 2 MHz. The LNA amplifies the received backscattered power P_r and a commercially available open-source universal software radio platform (USRP) [15] demodulates the data. The base-band data, V_{bb}, are filtered and sampled by an analog to digital converter (ADC) and contain $V_{I,n}$ and $V_{Q,n}$ signals from the Tunneling Tag. The raw data are recorded at 10 MSps, resulting in a Nyquist frequency of 5 MHz, and stored on a binary **.bin* file which can be read and processed using either MATLAB or GNU Radio. A Discrete Fourier Transform (DFT) is applied on the received signals at the frequency of interest f_m through a Goertzel filter performed on both the in-phase (I) and the quadrature (Q) channels of the receiver. Although the modulation scheme used for this project is relatively simple, more complex modulations, such as QAM [16], can be implemented using a combination of two or more tunnel diodes properly tuned and biased.

B. The Tunneling Tag

The 5.8 GHz Tunneling Tag consists of a TR (Fig. 3) connected to a tag antenna of gain G_t and a waveform generator that modulates, amplifies and backscatters the impinging CW through a biasing square wave of tunable voltage amplitude V_{pp} and frequency f_m. The tunnel diode used for this design is fabricated using rapid thermal diffusion

This article has been accepted for publication in a future issue of this journal, but has not been fully edited. Content may change prior to final publication. Citation information: DOI 10.1109/TWC.2018.2801803, IEEE Transactions on Wireless Communications

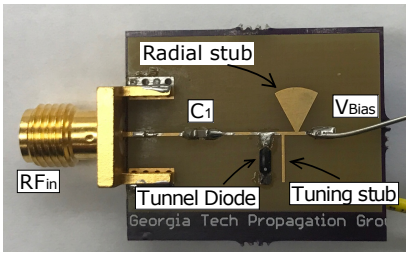

Fig. 3: Microstrip line structure of the fabricated Tunneling Reflector as in [12].

on Germanium substrate; since its electrical parameters (e.g.: junction capacitance) often vary from device to device, the tuning stub of the TR is used to compensate on these variations and allows fine tuning to the desired frequency of operation.

The Tunneling Tag switches between two states at a constant rate; the square wave can be represented as a Fourier series whose fundamental frequency is f_m, and has harmonics at integer multiples of this frequency. The tag can be tuned to other desired frequencies (e.g.: 915 MHz) by adapting the design topology in Fig. 3 and choosing appropriate parameters for tuning stubs, radial stub, and dc block capacitor.

C. Instrument Calibration

Since $V = V_I + jV_Q$ corresponds to the average voltage measured at the I and Q output ports of the microwave reader, a calibration procedure was necessary to identify the offset correction G (in dB) that needs to be taken out for measuring the correct amount of power $\widetilde{P}_r$ at the receiving antenna terminals:

$$\widetilde{P}_r = 10log_{10}\left(\frac{|V|^2}{2R}\right) + 30 - G, \tag{7}$$

with G being the offset correction and R = 50 Ω being the receiver impedance. The calibration procedure consisted in measuring an RF signal of known amplitude through both the microwave reader and a spectrum analyzer; the difference between the two measures was identified as the offset correction G. Once the received power is both measured ($\widetilde{P}_r$) through Eq. 7, and estimated (P_r) through the link budget equation[3], the TR gains $\widetilde{G}_{TR}$ can also be measured:

$$\widetilde{G}_{TR} = 10log_{10}\frac{\widetilde{P}_r}{P_r} \tag{8}$$

D. The Field Test Campaign

Tests were conducted by varying the distances r between the reader and the Tunneling Tag. For each distance, different bias voltages V_{pp} were applied for two or more modulation speeds f_m. For this work, the setups in Table I were used, each characterized by different system parameters chosen to have on the Tunneling Tag low amounts of impinging powers P_t. Setup I generates a CW with P_T of only 0 dBm (1 mW) and an EIRP of 6 dBm (4 mW); it was used to test the tag backscattering capabilities for distances r between 25 m and 160 m. Setup II and Setup III transmit a CW of 22 dBm (158 mW) and EIRP of 28 dBm (0.63 W), but use different tag antennas; they were used to test the prototype when located at 650 m and 1.2 km respectively. P_T levels were measured by directly connecting the output of the reader to a spectrum analyzer; antenna gains were simulated and then verified through experimental tests; L_1 and L_2 define the losses of the cables connecting the transmitting and receiving antennas to the reader. All the *.bin* files collected during the measurement campaign are publicly available at the GitHub repository [14] for scrutiny and free use by other researchers.

[3]Eq. 2 is used to compare the performances of an ideal semi-passive transponder (M = 1) with those of a tunneling tag ($M = \widetilde{G}_{TR} > 1$).

TABLE I: Configurations of the Experimental Setups

	Setup I	Setup II	Setup III
P_T (dBm)	0	22	
G_{tx} (dBi)	6		
G_{rx} (dBi)	24		
G_t (dBi)	6		24
G (dB)	15	30	
L_1 (dB)	1.2		
L_2 (dB)	0.9		

IV. Achieved Ranges and Gains of the Tunneling Tag

The measurement campaign aimed to experimentally verify the capabilities of a Tunneling Tag in terms of achievable ranges and gains. Fig. 1 and Table II show and summarize the measurements done for this work.

Since the Tunneling Tag has a very high sensitivity, Setup I, characterized by a transmitting power P_T of only 0 dBm and a total EIRP of 6 dBm, was used to test the prototype communication capabilities up to 160 m. Tests at distance r from 25 m to 50 m were held at the *Van Leer* site. At the *Tech Green* site, backscattering tests were done with the tag located 70 m, 100 m and 160 m from the reader. For each distance r, the prototype was modulated with different bias voltages V_{pp} (from 60 mV to 68 mV, 2 mV step) and at the modulating frequencies f_m of 250 kHz and 1 MHz, respectively. For each test, the demodulated complex data $V_n = V_{I,n} + jV_{Q,n}$ were stored as *.bin* files and post-processed in MATLAB to calculate the average value $|V|$ and the received power $\widetilde{P}_r$ (Eq. 7).

Fig. 4, 5 and 6 display the symbol constellations on the IQ plots when the prototype is located at different distances r from the reader and modulates at 250 kHz and 1 MHz, respectively; the reader noise level is also shown. It is important to highlight that, for Figs. 4-6, the IQ-processing software plots only one half of the IQ plane and the calibration procedure mentioned in Sec. III-C was used to compensate the missing half.

The collected *.bin* files are processed to retrieve, through Eq. 7, the effective measured powers $\widetilde{P}_r$ at the ends of the receiving antenna. The $\widetilde{P}_r$ are reported in Fig. 7 for different biases V_{pp} and for modulations at 250 kHz and 1 MHz. These values are compared against the received powers P_r expected by an ideal semi-passive RFID tag (M = 1) not equipped with any TR. The Tunneling Tag performs particularly well when it is far away from the transmitter allowing communications

This article has been accepted for publication in a future issue of this journal, but has not been fully edited. Content may change prior to final publication. Citation information: DOI 10.1109/TWC.2018.2801803, IEEE Transactions on Wireless Communications

TABLE II: Field Test Locations.

Location Name	Reader Location	Farthest Tag Location	Distance (m)	Used Setup
Van Leer, roof top	Lat. 33° 46 32.63 N Long. 84° 23 48.95 W	Lat. 33° 46 32.72 N Long. 84° 23 50.79 W	25 to 50	Setup I
Tech Green	Lat. 33° 46' 26.38" N Long. 84° 23' 48.25" W	Lat. 33° 46' 26.39" N Long. 84° 23' 54.78" W	70 to 160	Setup I
GTPE, parking lot	Lat. 33° 46' 32.63" N Long. 84° 23' 48.95" W	Lat. 33° 46' 32.71" N Long. 84° 23' 23.41" W	650	Setup II
Viewpoint, Midtown	Lat. 33° 46' 32.63" N Long. 84° 23' 48.95" W	Lat. 33° 46' 41.14" N Long. 84° 23' 2.56" W	1200	Setup III

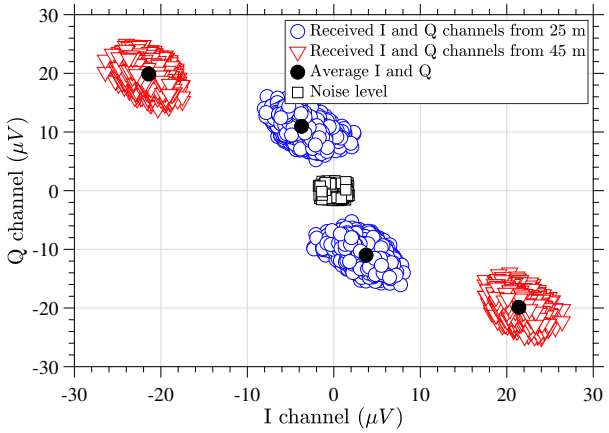

Fig. 4: IQ diagrams for the received base-band free-space backscattered signals on Setup I. V_{pp} = 60 mV, f_m = 250 kHz, r = 25 and 45 m.

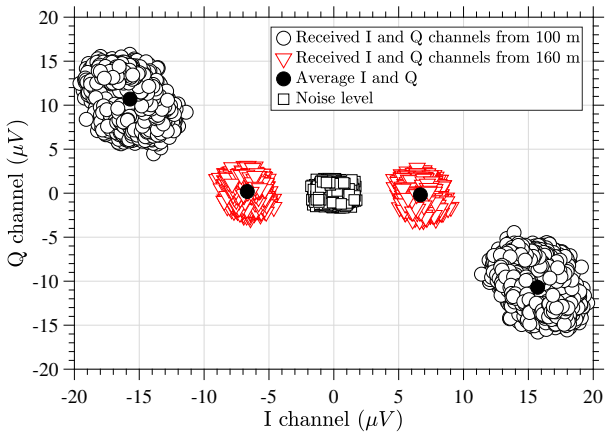

Fig. 5: IQ diagrams for the received base-band free-space backscattered signals on Setup I. V_{pp} = 60 mV, f_m = 250 kHz, r = 100 and 160 m.

at distances nowadays not yet possible for a backscattering technology. Moreover, longer distances (or lower powers) trigger better gains in the prototype; in fact, in Fig. 4 the voltage levels at 45 m are higher than the voltages measured at 25 m. A correct biasing influences the tag gains as well; in fact, better gains are observed for a 60 mV biasing voltage and a current of 340 μA. The gain $\widetilde{G}_{TR}$ of the prototype can be retrieved through Eq. 8 by comparing the measured received

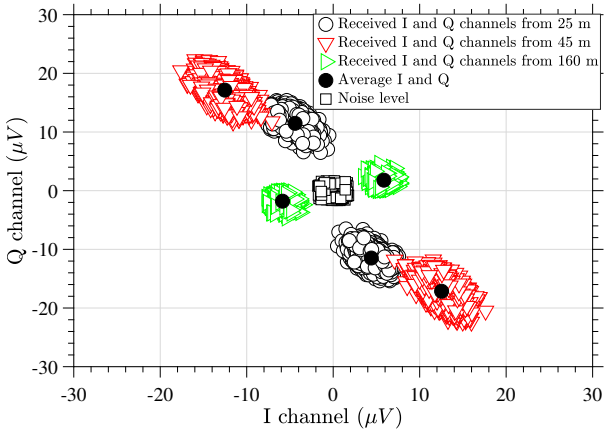

Fig. 6: IQ diagrams for the received base-band free-space backscattered signals on Setup I. V_{pp} = 60 mV, f_m = 1 MHz, r = 25, 45 and 160 m.

power $\widetilde{P}_r$ with the power P_r expected by an ideal semi-passive tag when free-space propagation is assumed. These values are summarized in Table III highlighting how the tag is beneficial for backscattering links between 35 m and 160 m. The impinging powers P_t were estimated through Eq. 1 and their influence on the TR gains $\widetilde{G}_{TR}(P_t)$ are shown in Fig. 8. It is important to point out that at these long ranges, the variability of propagation losses increases therefore, the accuracy of the assumed free-space propagation is reduced.

The data points obtained through the measurements campaign involving distance r between 25 m and 160 m were used to extrapolate a mathematical model that best describes the gains G_{TR} for impinging powers ranging between -80 dBm and -55 dBm:

$$G_{TR}(x) = a_1 e^{-\frac{(x-b_1)^2}{c_1}} + d_1 \quad (9)$$

with the coefficients $a_1 = 34.63$; $b_1 = -78.24$; $c_1 = 93.67$; $d_1 = 4$; and x being the power P_t, in dBm, impinging on the TR. The choice of Eq. 9 was made considering the trade-off between overfitting the model and reducing the root mean square error (RMSE) between the measured data and the predictive curve. Using higher order mathematical models, i.e. third/fourth order polynomials, would reduce the RMSE; however, it would also cause overfitting, making the predictions unreliable. Among various possibilities, the offset Gaussian function showed the best trade-off and provided a closed form expression that can be used in link-budget

This article has been accepted for publication in a future issue of this journal, but has not been fully edited. Content may change prior to final publication. Citation information: DOI 10.1109/TWC.2018.2801803, IEEE Transactions on Wireless Communications

TABLE III: Measured received powers and gains

Location	Distance (m)	Est. Power on tag P_t (dBm)	Est. Rx Power P_r (dBm)	Meas. Rx Power $\tilde{P}_r$ (dBm)		Tunneling Tag Gain $\tilde{G}_{TR}$ (dB)	
				250 kHz	1 MHz	250 kHz	1 MHz
Van Leer, roof top	35	-67.8	-117.3	-105.4	-105.5	11.8	11.7
	50	-70.9	-123.5	-104.6	-104.5	18.9	18.9
Tech Green	70	-73.8	-129.3	-98.7	-99.1	30.6	30.2
	100	-76.9	-135.5	-99.4	-103.3	36.1	32.5
	160	-81	-143.7	-108.5	-109.2	35.2	34.4

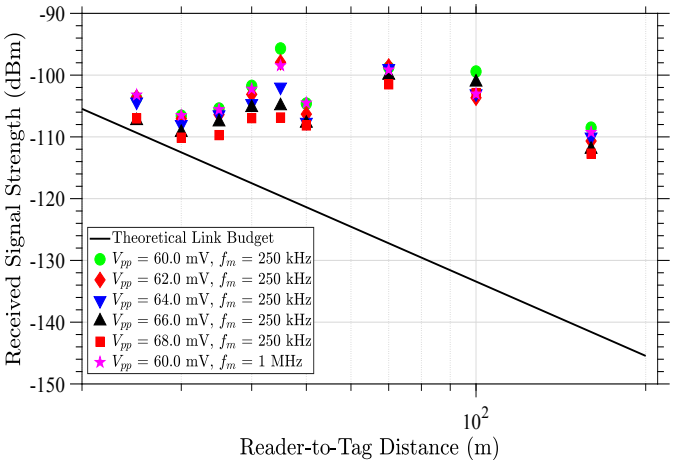

Fig. 7: Received signal strengths $\widetilde{P}_r$ in free-space as function of distances r, biasing voltages V_{pp}, and modulation speeds f_m using Setup I (6 dBm EIRP). Results are compared against an ideal semi-passive link (M = 1 and no Tunneling Reflector) using the same configurations as in Setup I.

calculations. In Fig. 8, both the experimental gains $\widetilde{G}_{TR}$ and the trend of $G_{TR}(x)$ (Eq. 9) are compared. The abrupt gain improvement at low values of P_t powers can be observed.

V. Gain Model Validation and Modulation Errors

To test the accuracy of the mathematical model (Eq. 9) in predicting the TR gains G_{TR}, backscattering tests were held with the Tunneling Tag placed at 650 m and 1.2 km away from the reader (Fig. 1). Setup II and III in Table I were used to have impinging RF powers on tag P_t ranging between -80 dBm and -55 dBm.

A summary of the results in shown in Table IV. The received powers $\widetilde{P}_r$ were measured from the reader and compared with the received powers P_r (Eq. 2) extrapolated when using an ideal semi-passive tag (M = 1) in free-space. The gains $\widetilde{G}_{TR}$ were retrieved through Eq. 8 and compared with the G_{TR} computed through Eq. 9. The accuracy of the mathematical model in predicting the gains is evident; in fact, the TR gains both measured $\left(\widetilde{G}_{TR}\right)$ and estimated (G_{TR}) are the same at both 650 m and 1.2 km.

Finally, the MER defined in Eq. 6 can be used to estimate the SNR ratio of the communication link between the reader and the Tunneling Tag; as shown in Fig. 9, this ratio is always above 10 dB. Nevertheless, it is important to highlight that the MER collectively captures the noise of the transmitter and the modulation errors of the tag.

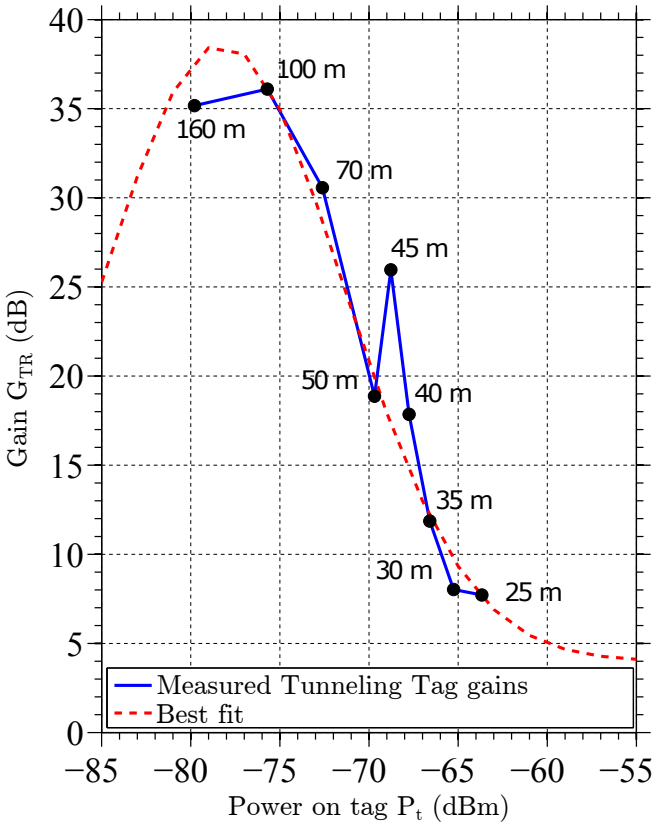

Fig. 8: Comparing the measured Tunneling Reflector gains, $\widetilde{G}_{TR}(x)$, with the gain model G_{TR} expressed through Eq. 9. The model is valid for RF powers P_t ranging between -80 dBm and -55 dBm.

TABLE IV: Comparing Gains: Measures *vs* Model

	Distance (m)	
	650	1,200
P_t (dBm)	-71.2	-58.5
1-way Path Loss (dB)	-104	-109.3
P_r (dBm)	-146.1	-120.7
$\widetilde{P}_r$ (dBm)	-121.8	-116.5
G_{TR} (dB)	24.3	4.53
$\widetilde{G}_{TR}$ (dB)	24.2	4.2

The discussion shown so far highlights some important achieved results: first, the prototype has shown a very low sensitivity, allowing it to work with impinging powers P_t as low as -81 dBm (Table III). Second, the Tunneling Tag is able to backscatter at distances as high as 160 m thanks to the added gains provided by the tunneling effect. The tag performed significantly better than any ideal passive and semi-

This article has been accepted for publication in a future issue of this journal, but has not been fully edited. Content may change prior to final publication. Citation information: DOI 10.1109/TWC.2018.2801803, IEEE Transactions on Wireless Communications

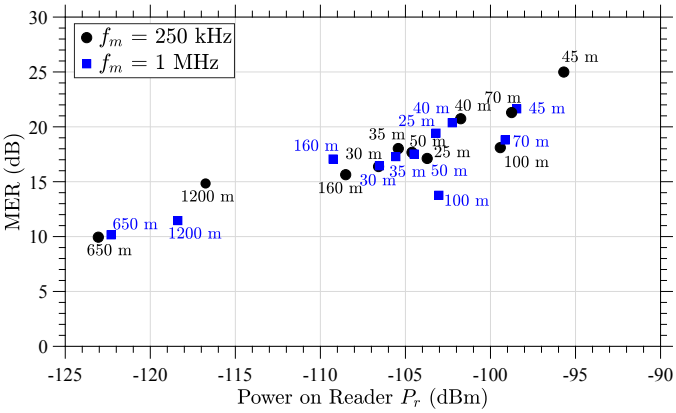

Fig. 9: Modulation Error Ratios (MER) for each measure of the test campaign.

passive tags equipped with the same antennas and operating at 5.8 GHz (Fig. 7). Third, it can reach tunneling gains as high as 36 dB and it performs better at longer distances when the impinging RF power P_t is below -70 dBm (Fig. 8). Finally, the plethora of collected data allowed to outline and validate a gain model for the Tunneling Tag (Eq. 9).

VI. A Link Budget Designer Tool

The successful measurement campaign described in the previous sections provided a valuable data set that demonstrated the capabilities of a Tunneling RFID Tag in achieving long communication ranges at 5.8 GHz and brought to the development of a tool assisting a system engineer in designing free-space long-range backscattering communication links.

The tool was developed in MATLAB and it incorporates the gain model of Eq. 9; its source code is available for use, test and improvement on Github [14]. A system engineer can set the desired ranges and frequencies as inputs and the tool gives as outputs the required system parameters that will establish the desired link when a Tunneling Tag is used. Four system parameters were identified: the transmitting power $P_T \in$ [-20, 30] dBm, the transmitting antenna gain $G_{tx} \in$ [0, 6] dBi, the receiving antenna gain $G_{rx} \in$ [0, 30] dBi, and the Tunneling Tag antenna gain $G_t \in$ [1.76, 14] dBi.

A. Testing Scenarios

Several scenarios that would benefit from the use of a long-range backscattering link were identified to test the tool and compare the results with the currently available RFID technology. On a football field, players wearing Tunneling Tags can be monitored by a reader suspended at the center of the field; tags on commercial products in a warehouse can assist employees (or drones) to quickly locate them for shipment; long-range and low-powered RFID tags would improve the efficiency and the flexibility of current and future precision agriculture applications suffering from the lack of technical solutions. People, airplanes and vehicles could be easily monitored in university campuses, airports, and cities. For every chosen scenario, the tool provided the system parameters necessary to establish a communication link.

B. Long Range Backscattering

A list of the chosen scenarios, their radius and, for each of them, the system parameters provided by the designer tool are summarized in Table V for a backscattering configuration involving either a *co-located bistatic*[4] ($G_{tx} \neq G_{rx}$) reader or a *monostatic* ($G_{tx} = G_{rx} = G_x$) reader.

For the bistatic configuration, the choice of the system parameters was made by using the following criteria: preferences were given to tag antennas with the lowest gains G_t (e.g.: a short dipole 1.8 dBi; a half wave dipole 2.1 dBi; or a patch antenna 9 dBi) in order to reduce the tag size; a dipole was preferred as the reader transmitting antenna for its omnidirectional pattern that allows a uniform coverage of the entire area of interest; finally, a low transmitting power P_T was preferred to reduce the power consumption of the reader. The obtained results are summarized in Table V; up to 300 m, the tag requires a half wave dipole, while between 300 m and 1.5 km, a patch antenna is enough to establish the link. The highest required transmitting power P_T is 21.4 dBm, about 8 dBm below the maximum power of 30 dBm allowed by the FCC regulations [9]. Finally, at 2 km, a higher gain antenna (G_t = 11.7 dBi) is required on the tag. It is important to highlight that, for the longest range scenarios (university campus, crop field, airport and city), the use of more directive tag antennas would limit the coverage to 180° (or less) therefore, more than one antenna on the tag might be required for a 360° coverage.

For the monostatic configuration, the lowest transmitting powers P_T were preferred among the solutions provided by the designer tool. Although all the monostatic scenarios are possible (Table V), the reader antenna requires a certain directivity that prevents a 360° coverage of the area. A solution to this limit could consist in using a reader antenna with lower gain G_x and a tag antenna with higher gain G_t whose omnidirectional properties would be preserved through a retrodirective structure.

As an example, Fig. 10a details the advantages of using a Tunneling Tag (M = G_{TR}) versus an ideal semi-passive tag (M = 1) to establish a backscattering link in a university campus with a 700-meter radius when a reader with -110 dBm receiving sensitivity is used in a bistatic configuration. A range improvement of 1 order of magnitude can be observed.

The entire free-space coverage of all the scenarios listed in Table V is summarized in Fig. 10b. It is important to stress out that, since the Tunneling Tag model was proven to be valid for impinging RF powers P_t ranging between -80 dBm and -55 dBm, were taken into account only distances at which correspond these power levels. The benefit of a Tunneling Tag is here evident in the bistatic configuration: the added gain G_{TR} allows a significant range extension in scenarios where the use of 5.8 GHz backscattering communication would not be otherwise possible.

[4]A co-located bistatic configuration consists in using a reader with two distinct but close-by antennas for transmission and reception.

This article has been accepted for publication in a future issue of this journal, but has not been fully edited. Content may change prior to final publication. Citation information: DOI 10.1109/TWC.2018.2801803, IEEE Transactions on Wireless Communications

TABLE V: Required System Parameters for Free-space Scenarios when Using an RFID Reader and a Tunneling Tag at 5.8 GHz

Scenario	Radius	Co-located Bistatic Reader					Monostatic Reader			
		EIRP dBm	P_T	G_{tx}	G_{rx} dBi	G_t	EIRP dBm	P_T	G_x dBi	G_t
Town House	20 m	-7.8	-9.6	1.8	5	1.8	-7.5	-11.5	4	1.8
Football Field	50 m	0.8	-1		12		0.4		11.9	
Warehouse (e.g.: Amazon)	100 m	7.7	5.9		19		6.6		18.1	
Skyscraper	300 m	16.8	15		28		16.2		27.7	
University Campus	700 m	16.3	14.5			9	23.5		35	6
Crop Field	1 km	19.7	17.9		31.5		21.8	-13.2		
Airport	1.5 km	23.2	21.4		35		22.5	-12.4		9
City	2 km					11.7	23.5	-11.5		11

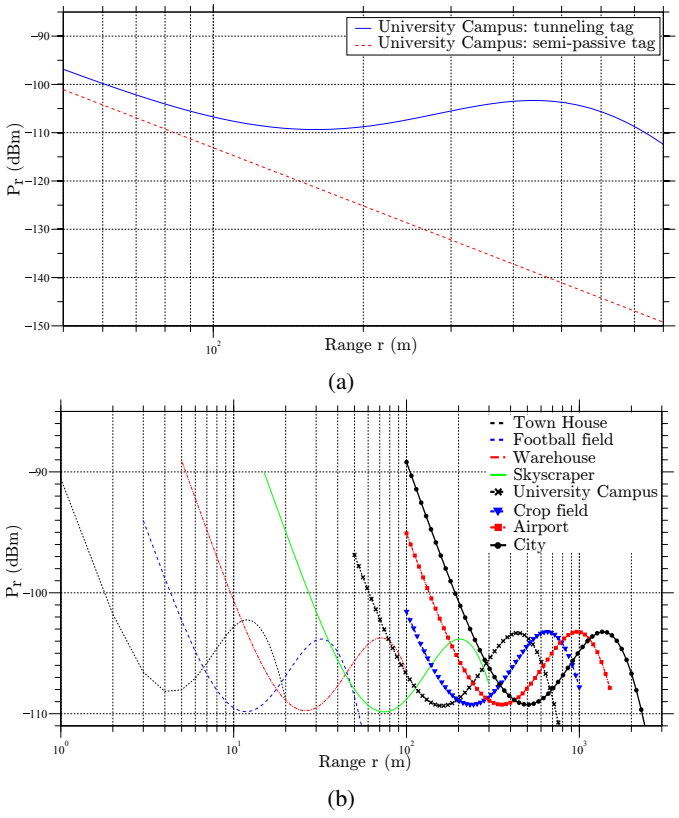

Fig. 10: (a) Comparing a 5.8 GHz backscattering bistatic link of 700 meter radius when an ideal semi-passive (M = 1) and a Tunneling Tag ($M = G_{TR}(x)$) are used; (b) whole coverage of different bistatic long-range scenarios. Free-space and a -110 dBm reader receiving sensitivity were assumed; similar results are obtained with monostatic configurations.

VII. Considerations on Power Consumption

The Tunneling RFID Tag here presented requires a certain biasing power to properly work. This requirement does not allow to identify the prototype as a passive transponder; nevertheless the consumed power is extremely low when compared to any other state-of-the-art RF wireless devices. Hence, a passive Tunneling Tag can be developed by adding a wireless energy harvesting module. The optimal biasing voltage (V_{pp} = 60 mV, I_{pp} = 340 μA) corresponds to a power consumption of only 20.4 μW that could be easily collected through wireless power harvesting or other power-scavenging techniques. This amount of biasing power, although very low, is enough to amplify very weak impinging RF signals whose amplitude is below -40 dBm. Moreover, since the modulation takes place by turning on and off the TR, only a fraction of this power is really used. Finally, since high modulation speeds are possible [17], the energy-per-bit expenditures are much lower than any other currently available technology. In fact, a modulating frequency f_m of 250 kHz and 7 MHz require $\left(E = \frac{V_{pp} I_{pp}}{f_m}\right)$ 81.2 μJ/bit and 2.9 pJ/bit, respectively.

Benefits for using a Tunneling Tag are also shared by the reader units. Thanks to the high sensitivity of the device, low impinging RF powers are enough to obtain backscattering modulation and amplification. FCC regulations allow up to 36 dBm (4 W) of transmit EIRP for backscattering readers operating at 5.8 GHz; nevertheless, the long-range experimental results shown in this work have been obtained for transmitting EIRPs as low as 6 dBm (4 mW) and the longest experimental range of 1.2 km was achieved by transmitting only 28 dBm (0.6 W) EIRP from the reader.

The low powers required by the Tunneling Tag prototype contribute, from both an economically and environmentally point of view, to a future with billions of wireless devices.

VIII. Conclusions

This work has presented a low powered Tunneling Tag achieving long-range backscattering communications at 5.8 GHz. The tag has a sensitivity of -81 dBm and achieved the experimental backscattering range of 1.2 km. The measurement campaign held at and nearby the Georgia Tech campus allowed to collect enough data to model the Tunneling Tag gains as a function of the impinging RF power P_t. Through this model, a tool to assist system engineers to design future long range backscattering systems was provided. Examples of free-space scenarios showed the possibility of covering wide areas by using dipole or patch antennas. The backscattering range of a 5.8 GHz RFID tag was increased by a factor of 10 when compared to an ideal semi-passive tag. Although it was designed and tested at 5.8 GHz, the prototype can be easily redesigned for the standard UHF frequencies at which even higher ranges can be covered.

Measurements showed a linear trend of the SNR for increasing impinging RF powers. SNRs above 10 dB were observed for modulation speeds up to 1 MHz. Moreover, the required biasing powers of only 20.4 μW widely contributes in the

This article has been accepted for publication in a future issue of this journal, but has not been fully edited. Content may change prior to final publication. Citation information: DOI 10.1109/TWC.2018.2801803, IEEE Transactions on Wireless Communications

reduction of power consumption that is currently drastically affecting the expansion of pervasive wireless nodes.

These results, by significantly reducing the power requirements while allowing great communication distances, demonstrate that the Tunneling Tag promises a new era for IoT wireless devices and backscattering applications. Finally, the provided tool can assist the design of long-range scenarios such as football fields, university campuses and cities that will benefit from the use of a Tunneling RFID Tag.

IX. Acknowledgements

The authors would like to thank Mrs. Siri G. Melkote and her family for the use of their apartment during the measurements campaign.

References

[1] IDC, *Intel*, united Nations.
[2] McKinsey Global Institute, "Strategy analytics M2M strategies advisory service," NYTimes.com.
[3] ATMEL. (Accessed Jan. 2018) Samb11. [Online]. Available: http://www.atmel.com/Images/Atmel-42426-SmartConnect-SAMB11-SOC_Datasheet.pdf
[4] Empire State Realty Trust, "Empire State building fact sheet," Accessed Jan., 2018. [Online]. Available: http://www.esbnyc.com/sites/default/files/esb_fact_sheet_4_9_14_4.pdf
[5] C. He, Z. J. Wang, C. Miao, and V. C. M. Leung, "Block-level unitary query: Enabling orthogonal-like space-time code with query diversity for MIMO backscatter RFID," *IEEE Transactions on Wireless Communications*, vol. 15, no. 3, pp. 1937–1949, March 2016.
[6] C. Boyer and S. Roy, "Invited paper - backscatter communication and RFID: Coding, energy, and MIMO analysis," *IEEE Transactions on Communications*, vol. 62, no. 3, pp. 770–785, March 2014.
[7] S. Grebien, J. Kulmer, F. Galler, M. Goller, E. Leitinger, H. Arthaber, and K. Witrisal, "Range estimation and performance limits for UHF-RFID backscatter channels," *IEEE Journal of Radio Frequency Identification*, vol. PP, no. 99, pp. 1–1, 2017.
[8] F. Amato, H. M. Torun, and G. D. Durgin, "Beyond the limits of classic backscattering communications: a Quantum Tunneling RFID tag," in *RFID (RFID), 2017 IEEE International Conference on*, May 2017.
[9] U.S. government publishing office, "Code of federal regulations," *FCC regulations, Title 47, Chapter 1, subchapter A*, vol. Part 15, Subpart C, no. 2, p. par.15.247, 10 2014.
[10] S. Hemour and K. Wu, "Radio-frequency rectifier for electromagnetic energy harvesting: Development path and future outlook," *Proceedings of the IEEE*, vol. 102, no. 11, pp. 1667–1691, 11 2014.
[11] C. H. P. Lorenz, S. Hemour, W. Li, Y. Xie, J. Gauthier, P. Fay, and K. Wu, "Breaking the efficiency barrier for ambient microwave power harvesting with heterojunction backward tunnel diodes," *IEEE Transactions on Microwave Theory and Techniques*, vol. 63, no. 12, pp. 4544–4555, Dec 2015.
[12] F. Amato, C. W. Peterson, M. B. Akbar, and G. D. Durgin, "Long range and low powered RFID tags with tunnel diode," in *RFID Technology and Applications (RFID-TA), 2015 IEEE International Conference on*, September 2015, pp. 182–187.
[13] J. Griffin, "High-frequency modulated-backscatter communication using multiple antennas," Ph.D. dissertation, Georgia Institute of Technology, Atlanta, 2009.
[14] F. Amato and H. M. Torun. (Accessed Jan. 2018) GitHub repository: 1kmRFID. [Online]. Available: https://github.com/francuz/1kmRFID
[15] Ettus Research. (Accessed Jan. 2018) USRP N200. [Online]. Available: https://www.ettus.com/product/details/UN200-KIT
[16] S. J. Thomas, E. Wheeler, J. Teizer, and M. S. Reynolds, "Quadrature amplitude modulated backscatter in passive and semipassive UHF RFID systems," *IEEE Transactions on Microwave Theory and Techniques*, vol. 60, no. 4, pp. 1175–1182, April 2012.
[17] F. Amato and G. D. Durgin, "Signal-to-Noise Ratio measurements for IoT communications with quantum tunneling reflectors," in *2016 IEEE World Forum on IoT*, December 2016.

Francesco Amato received his B.S. and M.S. in Telecommunication Engineering from the University of Roma Tor Vergata in 2006 and 2009, respectively and the Ph.D degree in Electrical and Computer Engineering from the Georgia Institute of Technology, Atlanta, GA (USA) in January 2017. He is currently a postdoctoral researcher at the Sant'Anna School of Advanced Studies (Pisa).
From 2009 to 2011 he worked at SES (Luxembourg) as Ground System Engineer. In 2012 he joined the Propagation Group at the Georgia Institute of Technology as Research Assistant and was a Research Intern at Intel Labs, Santa Clara, CA (USA). His current research interests include microwave photonics, backscatter radio communications, lidar systems and radars.
Dr. Amato was a mentor for the Opportunity Research Scholars Program of the Georgia Institute of Technology and received, among others, the Master Thesis Prize *Sebastiano e Rita Raeli* in 2009, the Fulbright Scholarship in 2012, the GoSTEM Fellowships in 2013 and 2014, the Best Student Paper Award of the IEEE International Conference on RFID-Technologies and Applications (RFID-TA) 2015, Tokyo (Japan), and the William Brown Fellowship in 2015. He is the organizing committee member for the 2017 and 2018 IEEE International Conference on RFID.

Hakki M. Torun (S'15) received his B.S. degree in Electrical & Electronics Engineering in 2016 from Bilkent University, Turkey. He joined Georgia Institute of Technology at Fall 2016 where he is currently a Ph.D candidate in Electrical and Computer Engineering under the supervision of Dr. Madhavan Swaminathan. His research interests include developing machine learning algorithms for system optimization and modelling with the applications in VLSI, power electronics, high speed channels and microwave systems.

Gregory D. Durgin joined the faculty of Georgia Tech's School of Electrical and Computer Engineering in Fall 2003 where he serves as a professor. He received the BSEE (96), MSEE (98), and Ph.D (00) degrees from Virginia Polytechnic Institute and State University. In 2001 he was awarded the Japanese Society for the Promotion of Science (JSPS) Post-doctoral Fellowship and spent one year as a visiting researcher with Morinaga Laboratory at Osaka University. He has received best paper awards for articles coauthored in the IEEE Transactions on Communications (1998 Stephen O. Rice prize), IEEE Microwave Magazine (2014), and IEEE RFID Conference (2016). Prof. Durgin also authored Space-Time Wireless Channels, the first textbook in the field of space-time channel modeling. Prof. Durgin founded the Propagation Group (http://www.propagation.gatech.edu) at Georgia Tech, a research group that studies radiolocation, channel sounding, backscatter radio, RFID, and applied electromagnetics. He is a winner of the NSF CAREER award as well as numerous teaching awards, including the Class of 1940 Howard Ector Outstanding Classroom Teacher Award at Georgia Tech (2007). He has served as an editor for IEEE RFID Virtual Journal, IEEE Transactions on Wireless Communications, and IEEE Journal on RFID. He also serves on the advisory committee on the IEEE Council for RFID (ComSoc Liaison). He is a frequent consultant to industry, having advised many multinational corporations on wireless technology.